Supplementary Information

Resolving the True Sodium Storage Sites in Hard Carbon: The Essential Role of Hydrogen Termination

Li Zhong[1,2,4], Yifang Li[1,2,4], Xingqiao Wu[1,2,4], Sean C. Smith[3], Shulei Chou[1,2,4], Xin Tan[1,2,4]**

[1] Institute for Carbon Neutralization Technology, College of Chemistry and Materials Engineering, Wenzhou University, Wenzhou, Zhejiang 325035, China.

[2] Zhejiang Provincial Key Laboratory of Advanced Battery Materials and Technology, Wenzhou University Technology Innovation Institute for Carbon Neutralization, Wenzhou, Zhejiang 325035, China.

[3] Integrated Materials Design Laboratory, Department of Materials Physics, Research School of Physics, Australian National University, Canberra, ACT 2601, Australia.

[4] Zhejiang-Australia International Joint Laboratory for Sodium-Ion Batteries, Wenzhou University Technology Innovation Institute for Carbon Neutralization, Wenzhou, Zhejiang 325035, China.

* Corresponding authors: Shulei Chou; Xin Tan

E-mail: chou@wzu.edu.cn; xintan@wzu.edu.cn

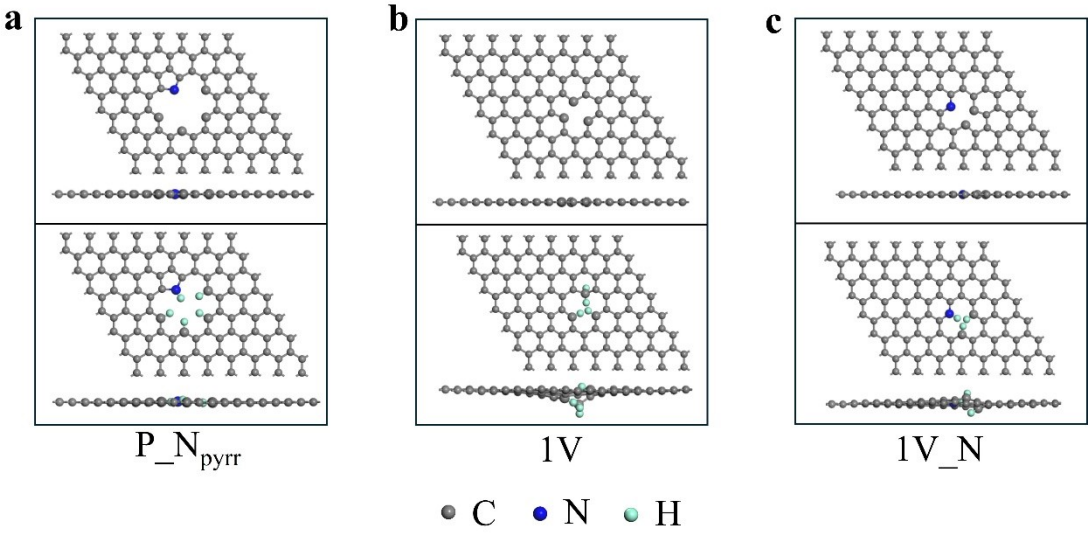

Figure S1. Structural models of HC before(top) and after (bottom) H-term. (a) P_N$_{pyrr}$, (b) 1V, and (c) 1V_N.

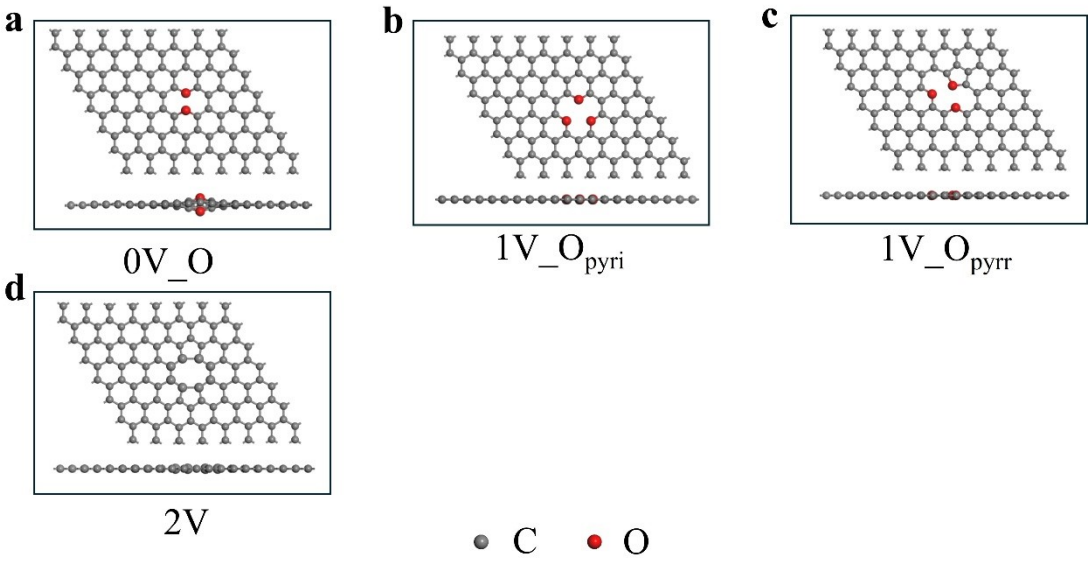

Figure S2. Structural models of HC. (a) 0V_O, (b) 1V_O$_{pyri}$, (c) 1V_O$_{pyrr}$, and (d) 2V.

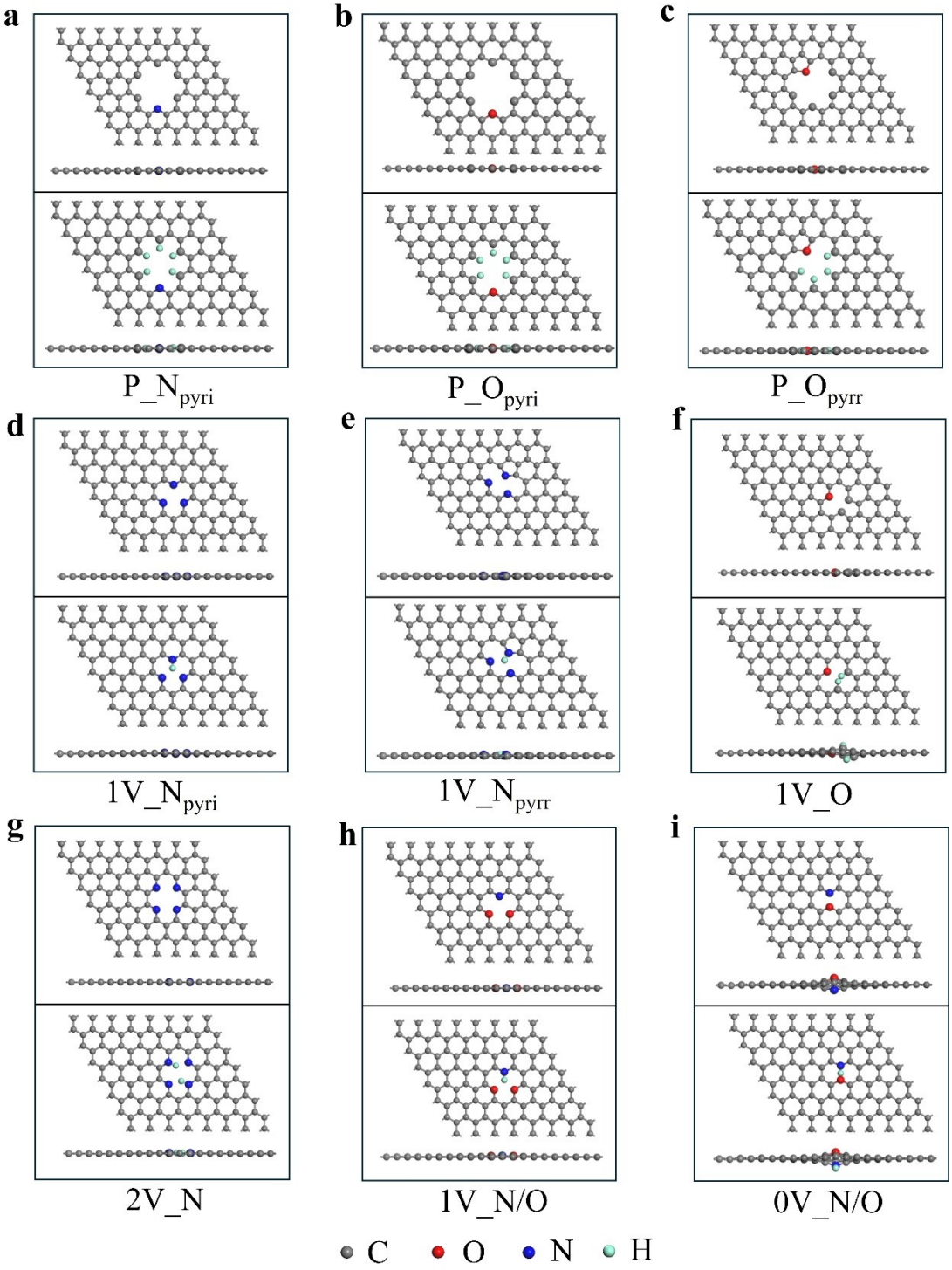

Figure S3. Structural models of HC before(top) and after (bottom) H-term. (a) P_N$_{pyri}$, (b) P_O$_{pyri}$, (c) P_O$_{pyrr}$, (d) 1V_N$_{pyri}$, (e) 1V_N$_{pyrr}$, (f) 1V_O, (g) 2V_N, (h) 1V_N/O, and (i) 0V_N/O.

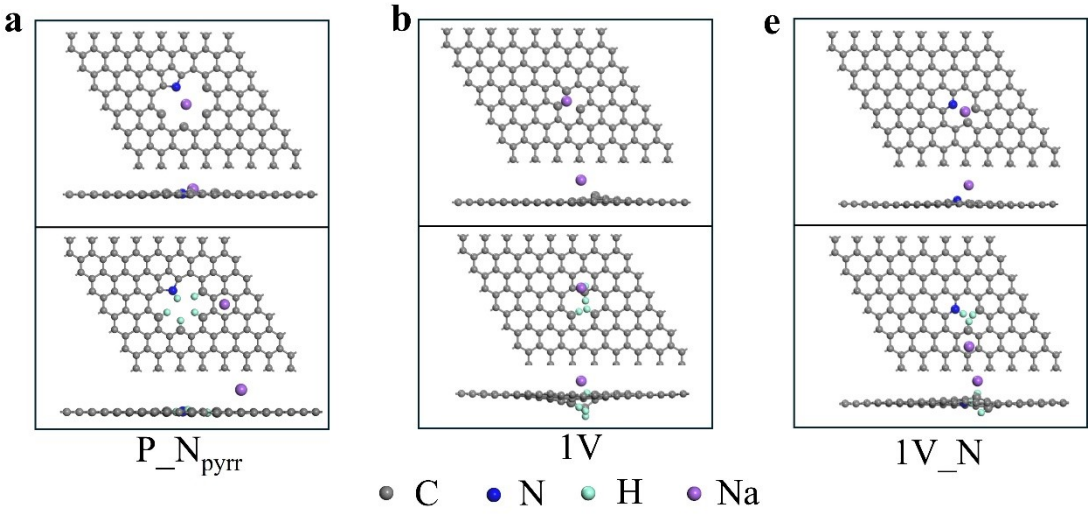

Figure S4. Structural models of Na adsorption on HC before (top) and after (bottom) H-term. (a) P_N$_{pyrr}$, (b) 1V, and (c) 1V_N.

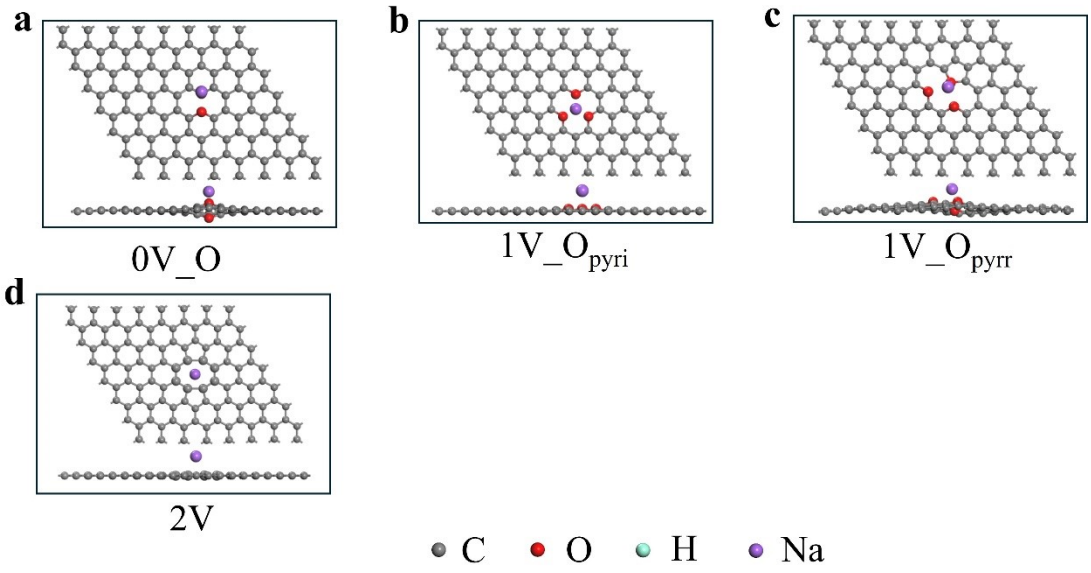

Figure S5. Structural models of Na adsorption on HC (a) OV_O, (b) 1V_O$_{pyri}$, (c) 1V_O$_{pyrr}$, and (d) 2V.

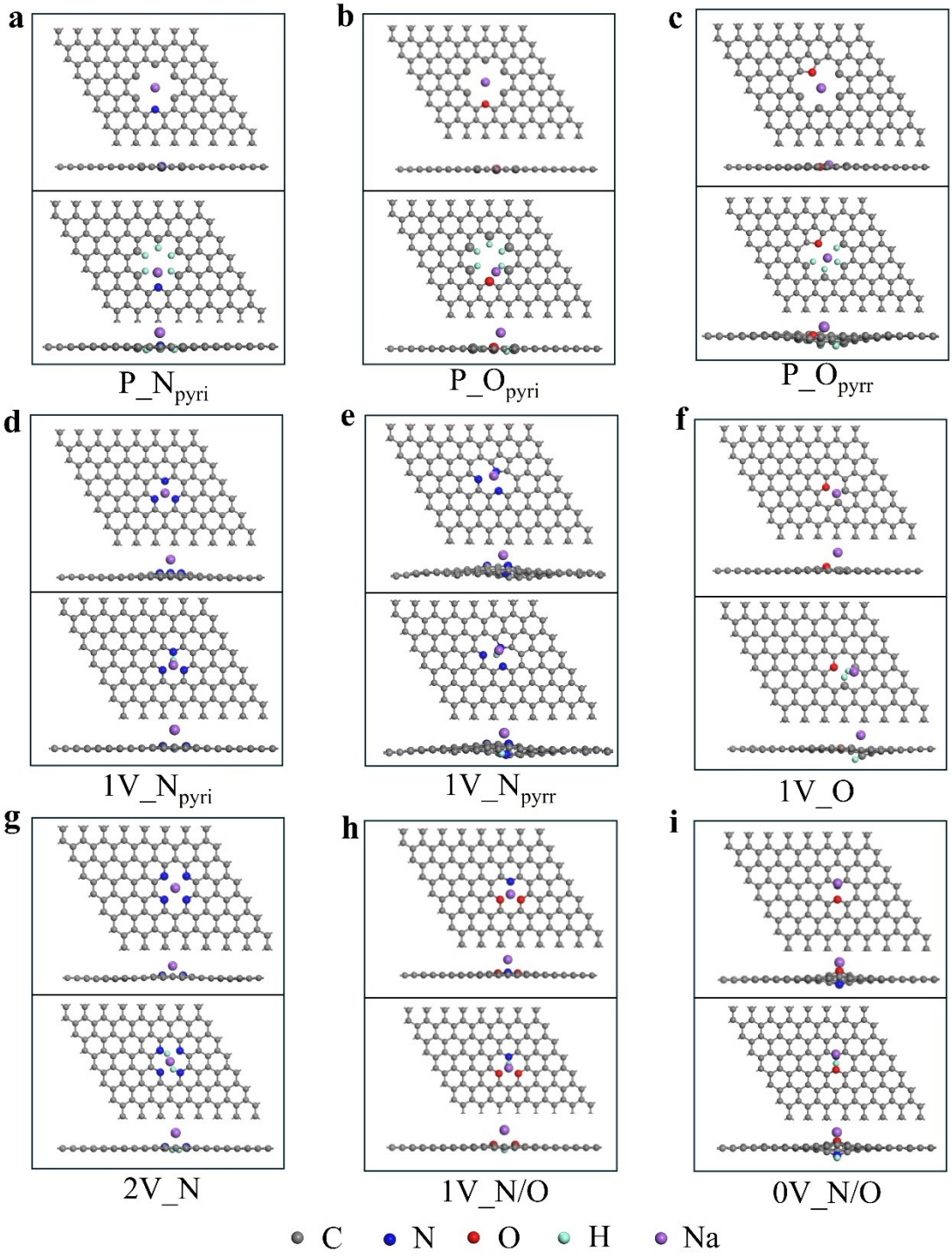

Figure S6. Structural models of Na adsorption on HC before (top) and after (bottom) H-term. (a) P_N$_{pyri}$, (b) P_O$_{pyri}$, (c) P_O$_{pyrr}$, (d) 1V_N$_{pyri}$, (e) 1V_N$_{pyrr}$, (f) 1V_O, (g) 2V_N, (h) 1V_N/O, and (i) 0V_N/O.

Table S1. E_{ads}(CDS, eV), E_{ads}(RDS, eV), and ΔE_{ads}(eV) values for the 16 HC structure models.

	E_{ads}(CDS, eV)	E_{ads}(RDS, eV)	ΔE_{ads}(eV)
P_N_{pyrr}	-2.77	0.32	3.09
P_N_{pyri}	-2.66	-0.09	2.57
P_O_{pyrr}	-2.46	0.08	2.54
P_O_{pyri}	-2.17	0.14	2.31
1V_N	-1.51	0.46	1.97
1V	-0.95	0.16	1.11
1V_N_{pyri}	-1.92	-0.09	1.83
2V_N	-2.24	0.04	2.27
1V_N_{pyrr}	-1.83	-0.59	1.25
1V_N/O	-0.39	0.41	0.79
0V_N/O	-0.54	0.17	0.71
1V_O	0.04	0.41	0.37
2V	-0.70	/	/
0V_O	0.17	/	/
1V_O_{pyri}	-0.01	/	/
1V_O_{pyrr}	-0.16	/	/

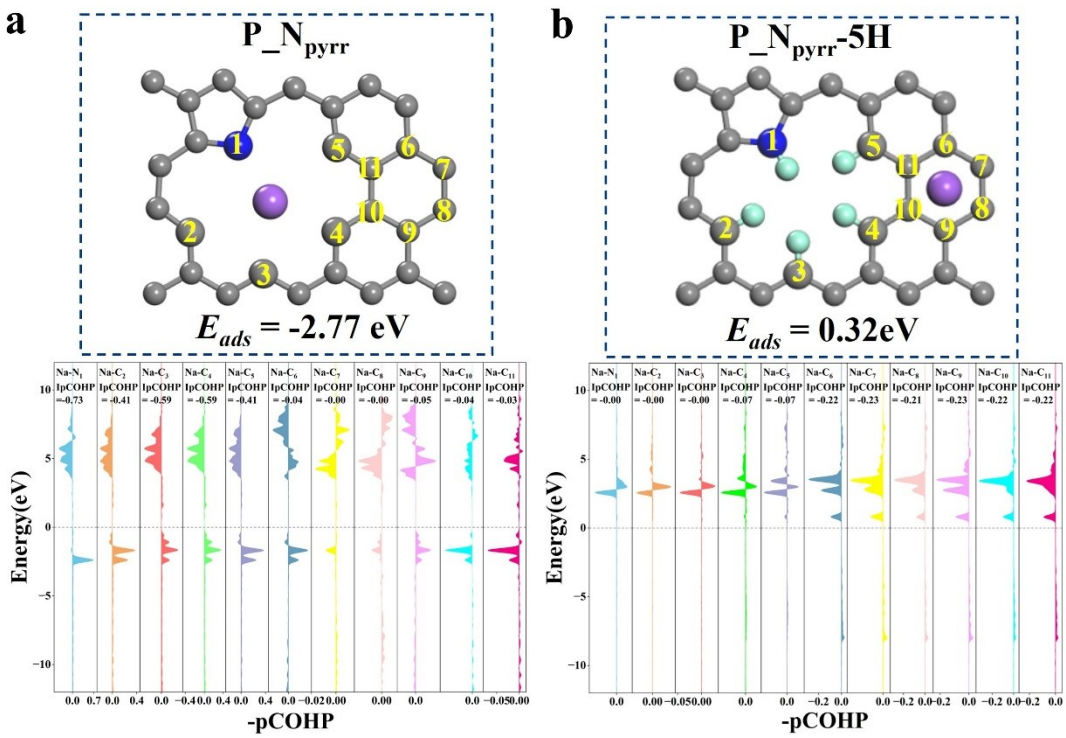

Figure S7. pCOHP and IpCOHP curves of ten Na-C and one Na–N bonds in (a) P_N$_{pyrr}$ and (b) P_N$_{pyrr}$-5H.

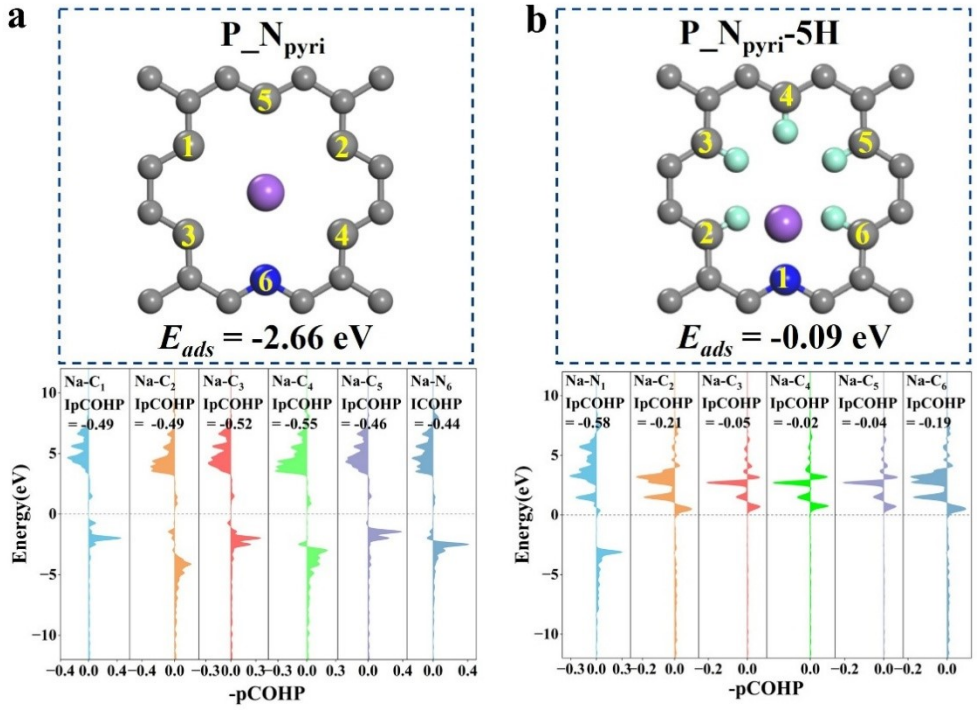

Figure S8. pCOHP and IpCOHP curves of five Na-C and one Na-N bonds in (a) P_N$_{pyri}$ and (b) P_N$_{pyri}$-5H.

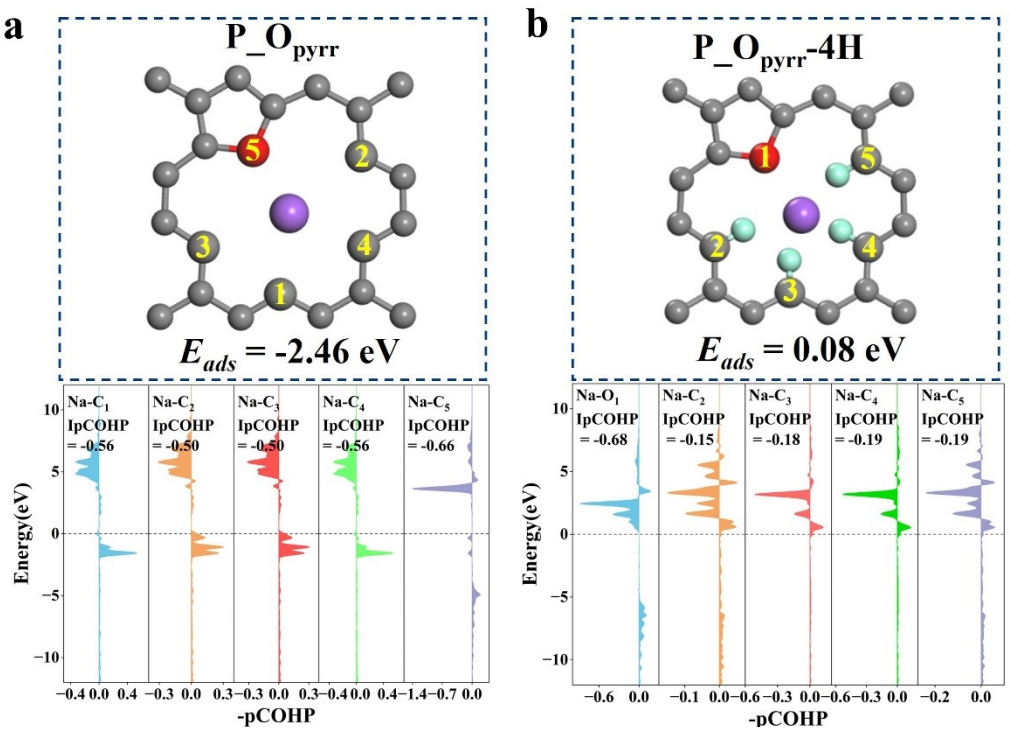

Figure S9. pCOHP and IpCOHP curves of four Na-C and one Na-O bonds in (a) P_O$_{pyrr}$ and (b) P_O$_{pyrr}$-4H.

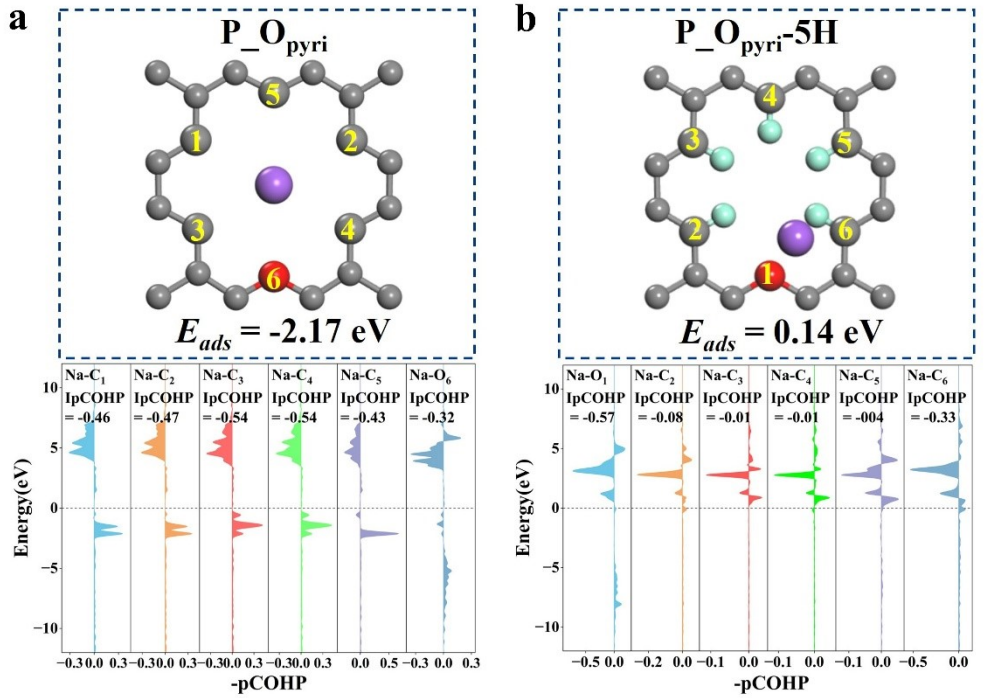

Figure S10. pCOHP and IpCOHP curves of five Na-C and one Na-O bonds in (a) P_O$_{pyri}$ and (b) P_O$_{pyri}$-5H.

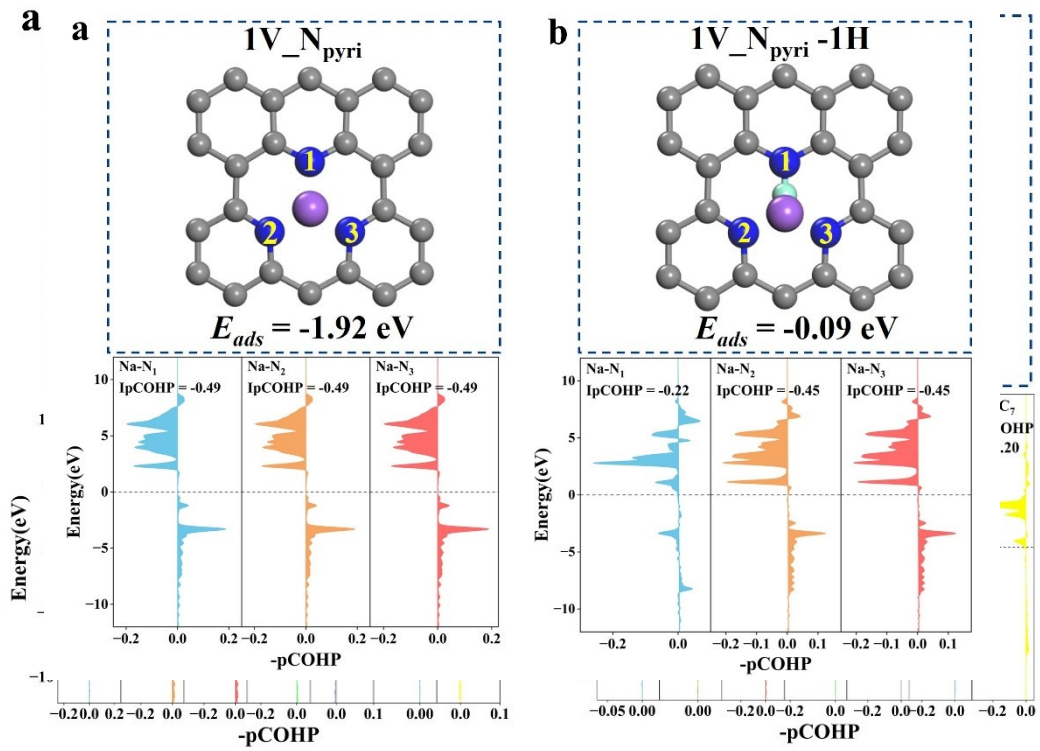

Figure S11. pCOHP and IpCOHP curves of one Na-N and six Na-C bonds in (a)1V_N and (b) 1V_N-3H.

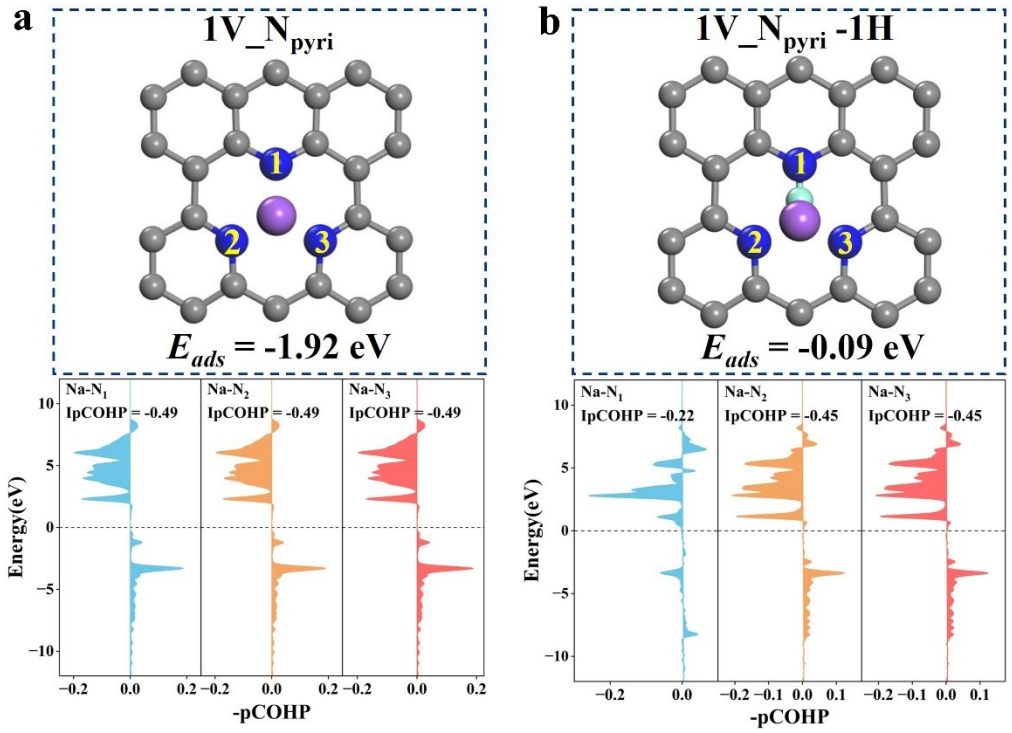

Figure S12. pCOHP and IpCOHP curves of three Na-N bonds in (a) 1V_N_{pyri} and (b) 1V_N_{pyri}-1H.

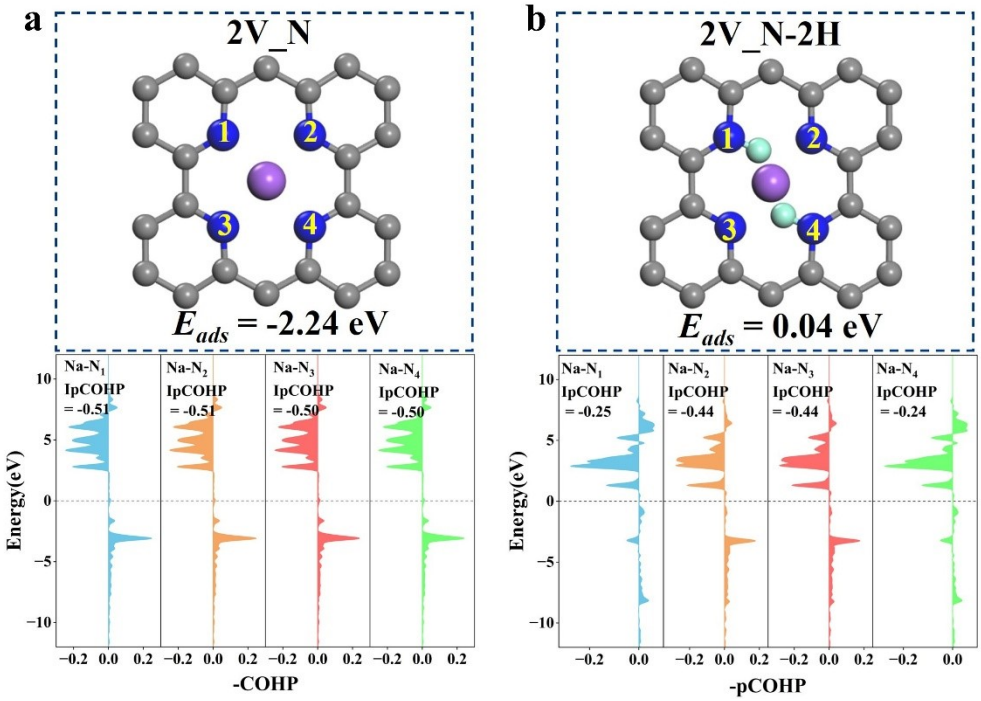

Figure S13. pCOHP and IpCOHP curves of four Na-N bonds in (a) 2V_N and (b) 2V_N-2H.

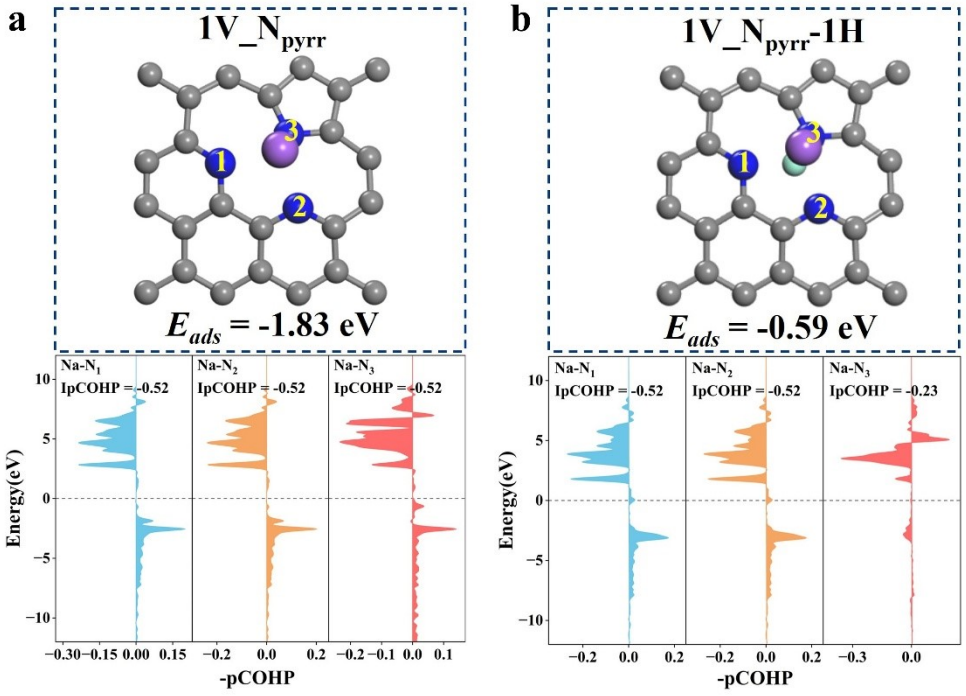

Figure S14. pCOHP and IpCOHP curves of three Na-N bonds in (a) 1V_N$_{pyrr}$ and (b) 1V_N$_{pyrr}$-1H.

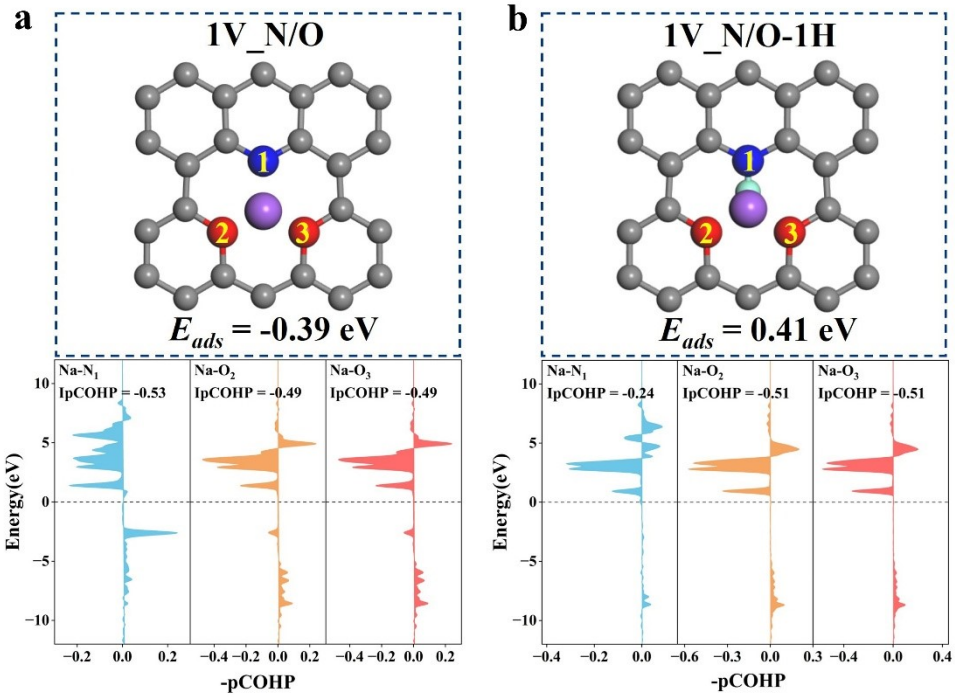

Figure S15. pCOHP and IpCOHP curves of one Na-N and two Na-O bonds in (a) 1V_N/O and (b) 1V_N/O-1H.

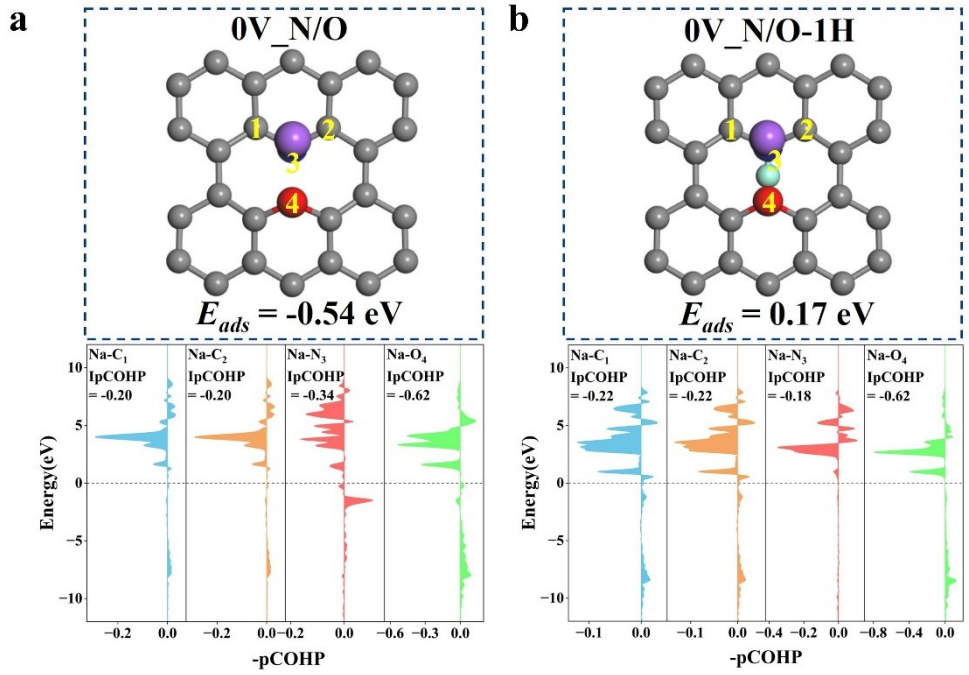

Figure S16. pCOHP and IpCOHP curves of two Na-C, one Na-N and one Na-O bonds in (a) 0V_N/O and (b) 0V_N/O-1H.

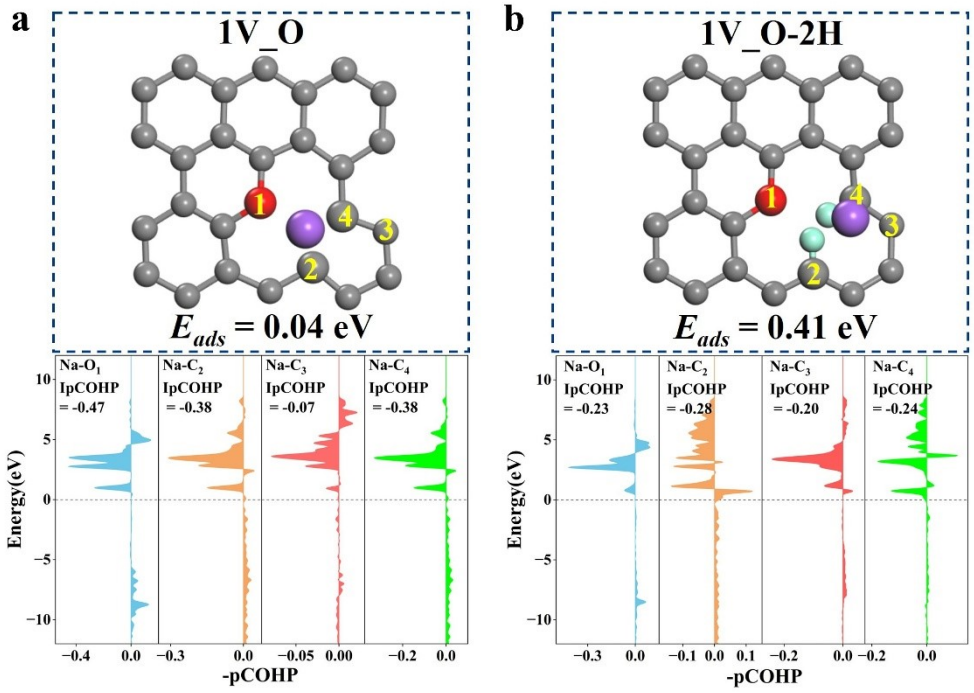

Figure S17. pCOHP and IpCOHP curves of three Na-C and one Na-O bonds in (a) 1V_O and (b) 1V_O-2H.

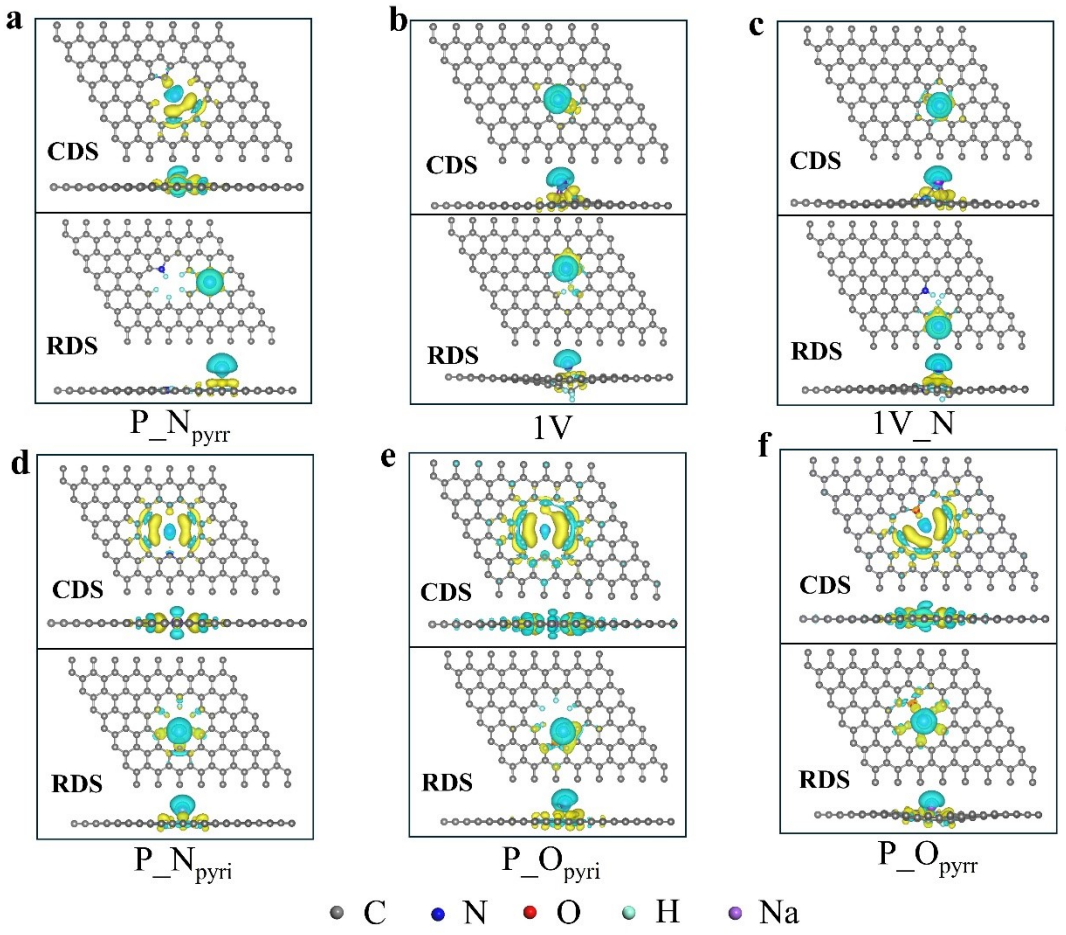

Figure S18. Differential charge density maps of Na adsorption on (a) P_N$_{pyrr}$, (b) 1V, (c) 1V_N, (d) P_N$_{pyri}$, (e) P_O$_{pyri}$, and (f) P_O$_{pyrr}$ (top and side views; isosurface = 0.002 e/Å^3).

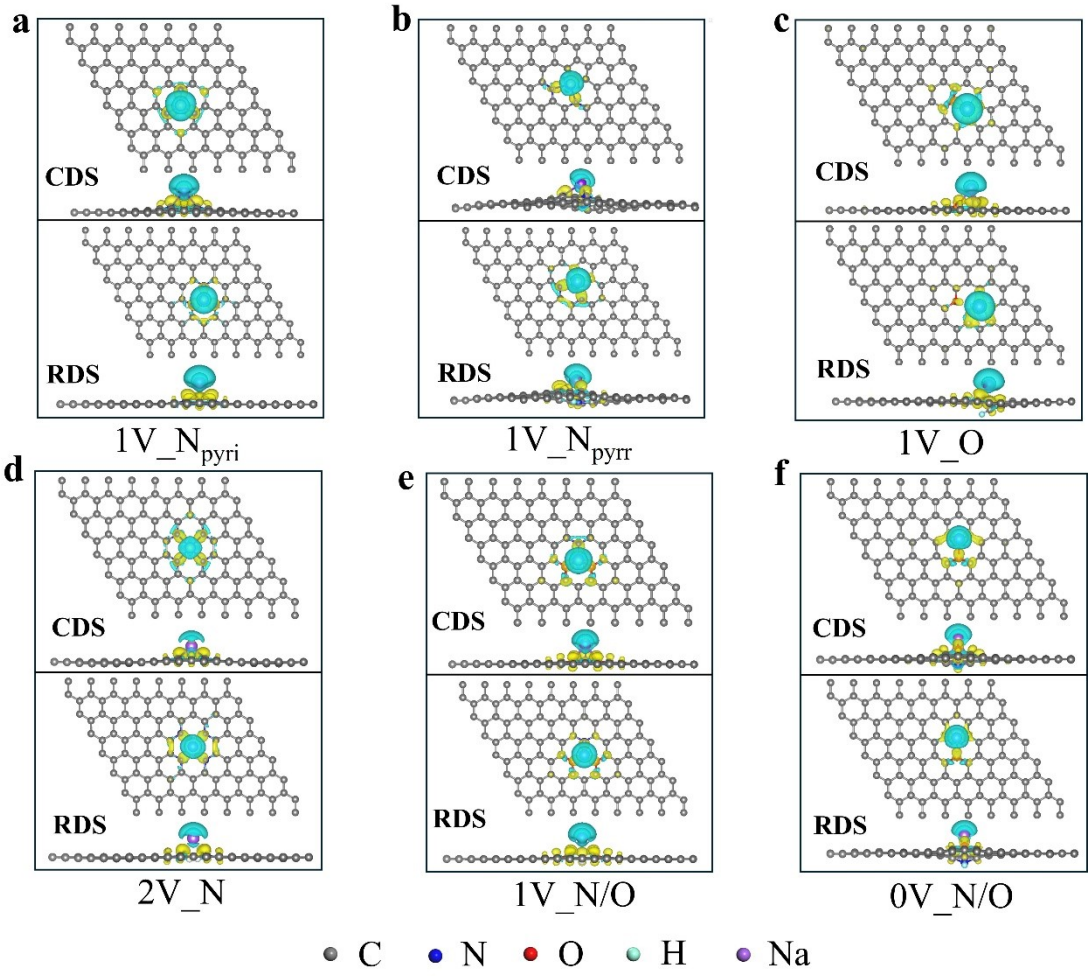

Figure S19. Differential charge density maps of Na adsorption on (a) 1V_N_{pyri}, (b) 1V_N_{pyrr}, (c) 1V_O, (d) 2V_N, (e) 1V_N/O, (f) 0V_N/O. (top and side views; isosurface = 0.002 e/Å^3).

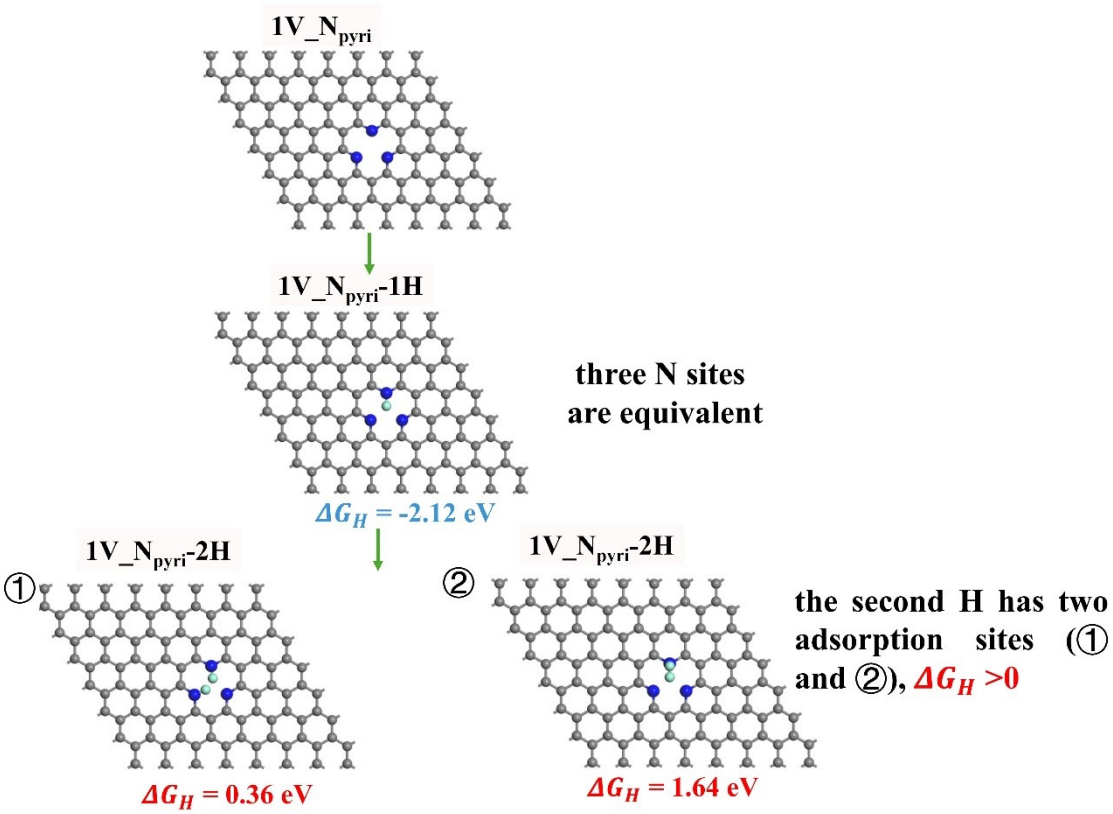

Figure S20. Schematic illustration of the stepwise H adsorption approach for determining the RDS configuration of 1V_N$_{pyri}$. The calculations reveal three equivalent pyridinic N sites for the first H addition. For the second H, although two candidate adsorption positions exist, both yield $\Delta G_H > 0$, confirming that only one H atom can be incorporated into the defect structure.

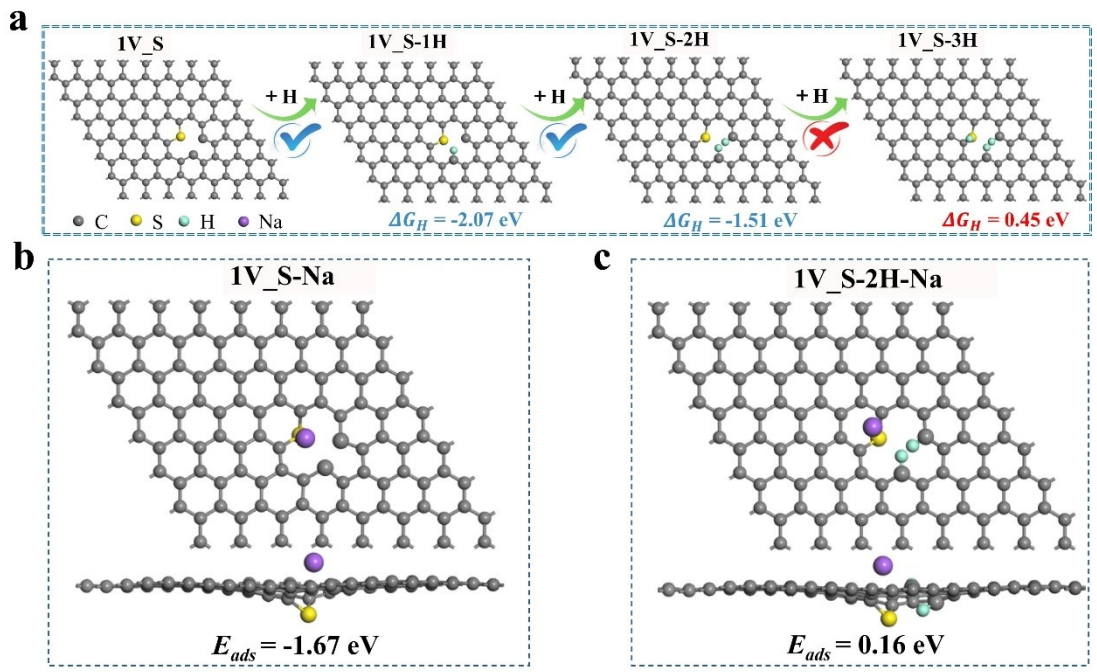

Figure S21. (a) Schematic illustration of the stepwise H adsorption approach used to determine the RDS configuration of 1V_S. Structural models of Na adsorption on (b) the unpassivated 1V_S defect and (c) the H-terminated 1V_S-2H configuration.

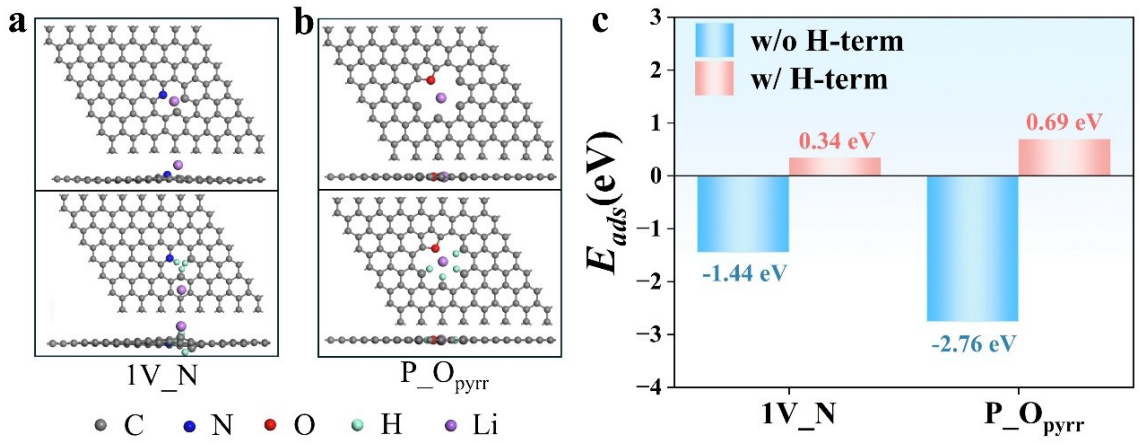

Figure S22. Structural models of Li adsorption on HC before (top) and after (bottom) H-term for (a) 1V_N and (b) P_O$_{pyrr}$, (c) Calculated E_{ads} for 1V_N and P_O$_{pyrr}$ defects using CDS and RDS models.

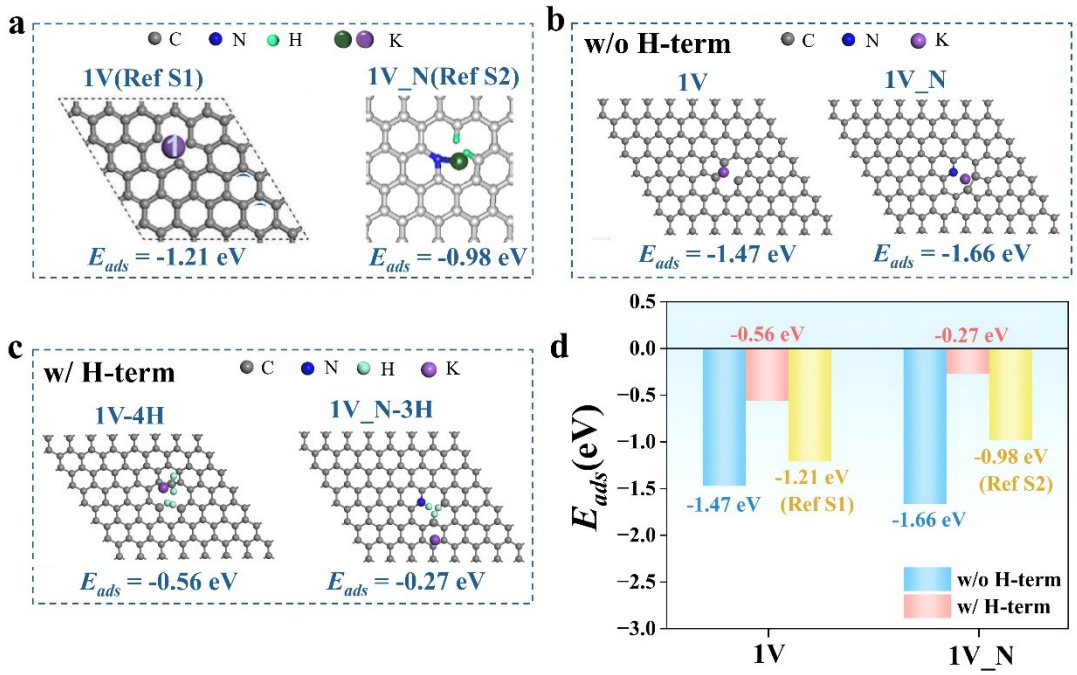

Figure S23. Structural models of K adsorption on 1V and 1V_N defects: (a) reference structures reported in the literature, (b) configurations without H-term, and (c) configurations with H-term. (d) Calculated E_{ads} for the 1V and 1V_N defects using the CDS and RDS models, shown in comparison with the reference values.[S1, S2]

References

S1. S. Zhao, K. Yan, J. Liang, Q. Yuan, J. Zhang, B. Sun, P. Munroe and G. Wang, *Adv. Funct. Mater.*, 2021, **31**, 2102060.

S2. Z. Zhu, Y. Men, W. Zhang, Y. Guo, X. Zeng, Y. Zhang, C. Tang, X. Li and Y. Zhang, *SusMat.*, 2025, **5**, e70017.